Orbit Stability in Three- and Four-Sector Cyclotrons

M. M. Gordon

Most of the work I am reporting on was actually done nearly a year ago and the results were presented informally at the annual ORNL Information Meeting last June. A fairly extensive account of this work can be found in the section on "Radial Stability" in ORNL Report 2648, "The Oak Ridge Relativistic Isochronous Cyclotron." This work is now, I believe, of historical interest principally in that it was the first work to indicate definitely the feasibility of the 3-sector medium-energy cyclotron as far as orbit stability considerations are concerned. Since that time a considerable amount of this kind of work has been done by those groups interested in the 3-sector machine, for example, that just reported by Blosser. There is no longer any doubt about the orbit stability of the 3-sector, weak-spiral cyclotron. As a result, this type of machine now appears more promising than the 4-sector (tight-spiral) machine for the medium energy region.

Let me explain briefly how we came to be involved in this work. Welton has for some time now been interested in the theoretical problems associated with a high energy proton cyclotron and under his direction a variety of Oracle computer codes have been developed for solving these problems. While I was at ORNL last year, most of the work we did was for an 8-sector machine which would start out in the center with four sectors. An alternative possibility was a 6-sector machine starting out with three sectors in the center. Both would accelerate protons up to the integral resonance $\nu_r = z$ which comes at 800 to 850 Mev for the 8-sector machine and at about 100 Mev less in the 6-sector one. The disadvantage of the lower energy in the 6-sector case is counter balanced by the resultant decrease in size and cost. Just about a year ago we began to worry about the various problems associated with the central, low energy, region of the big machine. Here we were faced with the question of orbit stability near $\nu_r = 1$ in either geometry. (Let me note, however, that conditions at the center of a big machine are quire different from those of the lower energy machines.)

Experience with the ORNL 4-sector electron model, as well as the Harwell calculations, have amply demonstrated the dangers of the third-integral subharmonic resonance $\nu_r = 4/3$. These results, together with the calculations done by Stahelin at Illinois, made us quite wary of the $\nu_r = 3/3$ resonance which would be encountered at the center of a 3-sector machine. Since the facilities were readily available we made some orbit studies with the Oracle computer to check into this matter ourselves. The high degree of orbit stability we discovered was somewhat surprising. The apparent cause of this stability was the fact that the $(\nu_r - 1)$ values were considerably higher than would be expected from the usual smooth-approximation formula. This effect was particularly marked in the 3-sector case and was the first indication we had that a 3-sector machine might, after all, have adequate orbit stability near its center.

It was just at that time when Cohen and Blosser began working on the basic design for the medium energy cyclotron, now dubbed the ORIC. They were embroiled in an argument over the relative virtues of the 3- and 4-sector geometries, and the crucial point of contention was orbit stability. Armed with the above mentioned results we stepped into the argument and suggested working some orbit studies with the computer which might help resolve the stability problem. It is the results of these first preliminary orbit stability computations that I will present today.

MEDIAN PLANE MAGNETIC FIELD:

$$B(r,\theta) = \frac{1}{\sqrt{1-r^2}}\left[1 + f(r)\cos 4(\theta - 24r)\right]$$

FLUTTER:

$$f(r) = f_0\left(\frac{r^2}{r^2+a^2}\right)^2$$

$$f_0 = 0.167;\ a = 0.018$$

LENGTH UNIT:

$$C/\omega_0 = 280 \text{ in.}$$

Fig. 50. Median plane magnetic field, for four-sector tight-spiral machine (N^{4+} ions).

The ORIC is designed to accelerate a variety of ions from protons on up to heavy ions. We chose N^{4+} ions for these first studies since their large mass results in ν_r being quite close to unity, according to the smooth approximation, over the entire energy range of the machine. Thus, we felt that if nonlinear orbit instability were a problem, it would show up most markedly in the case of nitrogen ions.

We consider first the results obtained for the 4-sector geometry. In Figure 50 we have the median plane field B (r,θ) used in these computations. The sinusoidal form of the flutter field was required to fit in with the available computer code. The flutter f (r) and spiral $\zeta(r)$ were chosen by Cohen to fit what were thought would be the conditions in the machine, using as a guide the model magnet studies and computations of Stahelin at Illinois. This is what we would call a weak-flutter, tight-spiral machine. The unit of length is the so-called cyclotron unit (here 280 in.) and the particles are accelerated out to an r-value of about 0.11. Thus, the total angle of rotation of the spiral is about 2.64 radians or 150°. The linear Archimedean spiral could not extend all the way in to R = 0, but we can assume that it is cut off. The form of f (r) used seems to fit the data quite well; the parameter α is comparable to the magnet gap. Note that f(r) goes to zero at the center as r^4, as it should for a 4-sector geometry. The form of the average field $(1 - r^2)^{-1/2}$ is what one would expect for zero flutter; since the flutter is so small here, it should suffice.

We took this field and ran it through the "equilibrium orbit" code about which you hear this morning. Some of the resultant data are shown in Figure 51. Here p is the momentum in MC units, E_k is the energy in Mev, t is the rotation period in units of the rf period, ν_z is the axial focusing frequency, ν_r is the actual radial oscillation frequency, and ν_r^0 is that obtained from the smooth approximation. Let us note first that the degree of isochronism is adequate (i.e., t = 1). Next we note that the values of ν_z climb with increasing energy. This increase comes about from the fact that the same flutter - spiral must focus both protons and N ions in this machine while the field index, k, is much smaller for the heavy ions. The larger values of ν_z are actually undesirable because of the dangers of the coupling resonance $\nu_r = \nu_z$, as we shall show later. Finally we note that the last two columns of Figure 51 show that $(\nu_r - 1)$ is actually much larger than the smooth approximation values, an effect which is even more pronounced for the 3-sector geometry as has already been reported several times today.

P	E_k	t	ν_z	ν_r	ν_r^0
0.020	2.6	0.9998	0.0403	1.0011	1.0002
0.045	13.0	0.9992	0.1581	1.0038	1.0010
0.070	33.0	0.9991	0.2635	1.0082	1.0025
0.095	59.0	0.9991	0.3653	1.0147	1.0045
0.120	94.0	0.9991	0.4660	1.0230	1.0072

Fig. 51. Orbit parameters for 4S-TS machine.

At this point, let me pause to interject a few remarks on analytical formulas for calculating ν_r. In the fall of 1957, I had made a rather painstaking analytical calculation to derive an

accurate formula for ν_r. The motivation for this work came from our studies of the big machine where we found that the energy at which $\nu_r = 2$ depended quite critically on the details of spiral and flutter assumed; I wanted some analytical guide in understanding our computer results. I used the results of a variational method for determining the form of the equilibrium orbit which I had worked out in the Spring of 1957. This method has the advantage of reducing the problem to straight-forward algebra as well as divorcing the results from the determination of other momentum as a function of radius.

The form of the median plane field used was:

$$B(r,\theta) = B_o(r) + B_1(r) \cos N[\theta - \zeta(r)]$$

with B_o, B_1, and ζ arbitrary. So I carried through the calculation of ν_r carefully keeping all terms that could contribute to the result to order $(1/N)^2$; I obtained

$$\nu_r^2 = 1 + k_o + (f^2/2N^2)\,[k_1^1 + k_1^2 + 5\,k_1 - k_o\,k_1 + 3\,k_o\,T^2 + 3\,T^2 + 3 + f^2\,(1/2\,k_1 + 1/2\,k_1\,T^2 - 2 - 3/8\,T^2 - 1/8\,T^4)]$$

Where:

$$f = B_1/B_o$$

$$T = R\,(d\zeta/dr)$$

$$k_o = (r/B_o)\,(dB_o/dr)$$

$$k_1 = (r/B_1)\,(dB_1/dr)$$

$$k_1^1 = (r^2/B_1)\,(d^2B_1/dr^2).$$

All quantities are evaluated at $r = R$, the mean radius of the equilibrium orbit. This equation checked quite well over results for the 8-sector machine and I put it aside. Just recently I thought of checking this equation against the results of our 3- and 4-sector computer calculations of ν_r. To do this I had to make an important change in the formula to take into account the closeness of ν_r to $(N/2)$. This has the effect of greatly enhancing the alternating gradient effect. The resulting increase in ν_r^2 over and above that given by the formula above is:

$$\Delta\nu_r^2 = A/(N^2 - 4\nu_r^2) - (A + C)/N^2,$$

where:

$$A = 1/2\,f^2\,N^2\,T^2 + 1/2\,f^2\,(k_1 + 3/2)^2$$

$$C = 2\,f^2\,T^2\,(1 + k_o).$$

Using these formulas we obtained a value of $\nu_r = 1.0010$ as against the computer value 1.0011 for the first p value in Figure 51.

OSCILLATION:

$$x = A\cos(\theta + \phi)$$

PERTURBATION:

$$16\,C\,x^3\cos 4\theta$$

FIRST-ORDER EQUATIONS:

$$\frac{dA}{d\theta} = CA^3 \sin 4\phi$$

$$\frac{d\phi}{d\theta} = (\nu_r - 1) + CA^2\cos 4\phi$$

INVARIANT:

$$H(A,\phi) = \tfrac{1}{2}(\nu_r - 1)A^2 + \tfrac{1}{4}CA^4\cos 4\phi$$

STABILITY LIMIT:

$$A_0 = \left(\frac{\nu_r - 1}{C}\right)^{1/2}$$

Fig. 52. Radial stability near $\nu_r = 4/4$.

Returning now to the question of orbit stability, we have in Figure 52 a very brief sketch of the nonlinear resonance theory as it applies to the $\nu_r^2 \cong 4/4$ case. (For simplicity, we have omitted the X^4 term.) The form of the "invariant" helps us understand the nature of the phase plots.

In Figure 53 we have the phase plots obtained at two energies for this 4-sector geometry. The nature and significance of these plots has already been discussed several times today. We start an orbit out with a given displacement x from the equilibrium orbit and plot to the values of p_x versus x once per sector as the trajectory is being computed by the Oracle. The fourfold symmetry in these plots is characteristic of the fourth-order subresonance (see Fig. 52). The angular separation between adjacent points is a measure of $(\nu_r - 1)$. The squarish closed figures represent stable orbits; the open figures unstable orbits. We can therefore estimate the range of stable amplitudes from examining these plots. Full scale in these plots represents a displacement of 4.4 inches. From these plots and additional ones at other energies we were able to conclude that amplitudes of oscillation up to about 2 inches would be stable in this machine provided the effects of acceleration were taken into account.

The calculations on the 3-sector geometry were made immediately after the 4-sector work just described. In Figure 54 we see the analytical form of the 3-sector magnetic field used for the computations. Here again this form was restricted by the available computer code. The specific parameters here were determined by Cohen to fit as well as possible the model magnet measurements of Blosser. The spiral here is quadratic in r and "weak"; that is, the total spiral angle reaches only

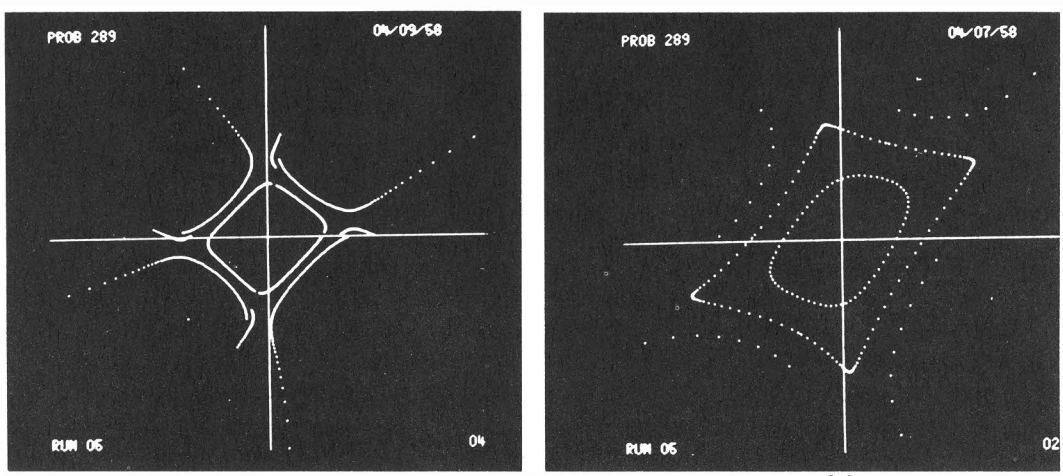

13 Mev-N^{4+} IONS 60 Mev-N^{4+} IONS

Fig. 53. Phase plots for four-sector machine.

MEDIAN PLANE MAGNETIC FIELD ($0.01 < r < 0.10$)

$$B(r,\theta) = \bar{B}(r)\left[1 + f(r)\cos 3(\theta - \zeta)\right]$$

$$\bar{B}(r) = 0.99383 + 0.00655\cos(57.8\,r)$$

$$f(r) = -0.096 + 14.0\,r - 91.8\,r^2$$

$$\zeta = 32.2\,r^2$$

Fig. 54. Analytical form of three-sector, weak-spiral machine for N^{4+} ions.

P	E_k	t	ν_z	ν_r	1 + k	f
0.02	2.6	1.0005	0.1420	1.0090	0.9930	0.147
0.03	5.9	1.0004	0.2140	1.0202	0.9887	0.241
0.04	10.0	1.0002	0.2676	1.0315	0.9887	0.317
0.05	16.0	0.9998	0.3043	1.0409	0.9952	0.374
0.06	23.0	0.9992	0.3293	1.0463	1.0074	0.414
0.07	32.0	0.9988	0.3503	1.0445	1.0210	0.434
0.08	42.0	0.9993	0.3754	1.0341	1.0304	0.436
0.09	53.0	1.0017	0.4086	1.0150	1.0302	0.420

Fig. 55. Orbit parameters for 3S-WS machine.

OSCILLATION:

$$x = A\cos(\theta + \phi)$$

PERTURBATION:

$$8\,C\,x^2\cos 3\theta$$

FIRST-ORDER EQUATIONS

$$\frac{dA}{d\theta} = C A^2 \sin 3\phi$$

$$\frac{d\phi}{d\theta} = (\nu_r - 1) + C A\cos 3\phi$$

INVARIANT:

$$H(A,\phi) = \tfrac{1}{2}(\nu_r - 1)A^2 + \tfrac{1}{3}CA^3\cos 3\phi$$

STABILITY LIMIT:

$$A_0 = \frac{\nu_r - 1}{C}$$

Fig. 56. Radial Stability near $\nu_r = 3/3$.

about 25° at the outside (r = 0.11). It is hard to gauge the behavior of the flutter, f, from its analytical form, but this will be made clearer in Figure 55, where numerical values are given. The behavior of the average field $\bar{B}$ is interesting. It falls off with increasing r for almost half the machine. This is due to the fact that f and df/dr are large and N = 3 is small here. The orbits are then quite triangular and the average field along the orbit is significantly greater than the value of the mean orbit radius.

The output of the equilibrium orbit code for this 3-sector field is shown in Figure 55. The explanation of the symbols is the same as that given above for Figure 51. The last column shows the values of the flutter, f. The values of 1 + k shown represent ν_r^2 in the smooth approximation limit, and it is seen that these values are less than unity over the first part of the machine where the average field is falling off. (With reference to Symon's comments, we wish to apologize for the misuse of the term "smooth approximation." What we have really done here is to neglect all terms of order N^{-2} in the formula given above for ν_r^2, and this implies not only the smooth approximation but also nearly circular orbits.) The actual values of ν_r shown are markedly greater than unity. The importance of the flutter gradient, as well as the flutter itself, can be seen from the way ν_r rises and then falls along with the corresponding f values shown. Using the formula given above for ν_r^2, we obtained at p = 0.03 the value $\nu_r = 1.0166$ compared with the value $\nu_r = 1.0202$ in Figure 55. The correction for the nearness of the $\nu_r = 3/2$ stop-band is very important here.

We consider now the results of the orbit stability calculations for the $\nu_r = 3/3$ resonance. The theory is summarized in Figure 56, the analogue of Figure 52 for the 4-sector case. We shall not discuss the theory here to save time. Such a discussion has already been given today by Smith.

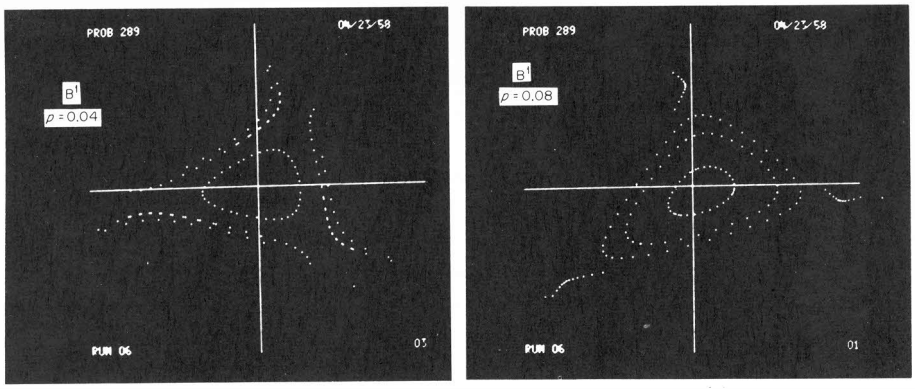

10 Mev-N^{4+} IONS 42 Mev-N^{4+} IONS

Fig. 57. Phase plots for three-sector machine.

In Figure 57, we have shown two of the phase plots obtained for this 3-sector field at two different energies. The interpretation of these plots has already been discussed in connection with Figure 53 and by the previous speakers. The scale of these plots is the same as that for Figure 53. Our conclusion from these results is that the 3-sector field gives orbit stability quite comparable to that of the 4-sector field as far as motion in the median plane goes.

This then was the first real evidence we had that a 3-sector machine would have adequate radial stability. The superiority of the 3-sector over the 4-sector machine with regard to orbit stability did not manifest itself, however, until we investigated the question of axial stability.

It is hoped that some type of regenerative beam deflection system can be worked out for this machine. Such a system seems almost imperative for 75-Mev protons. The essential feature of the regenerative process is a progressive build-up of large radial orbit displacements. The main problem we are faced with here is whether axial stability can be maintained during this process. The nonlinear coupling resonances, $2\nu_z = \nu_r$ and $2\nu_z = N - (N-1)\nu_r$ becomes active as the radial oscillation amplitude increases and may lead to axial instability.

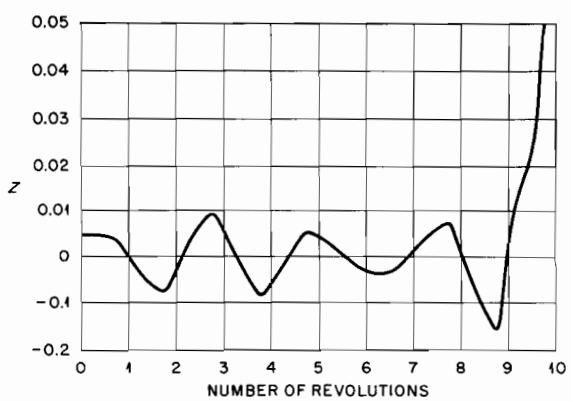

Fig. 58. Effect of coupling resonances on axial oscillations (for 4S-TS machine).

Using the 4-sector field discussed before (see Fig. 50) we made a computer run to check into this question. We chose an energy near the outside of the machine and started an orbit out with a radial displacement of about 2 in., which our previous work had shown would lead to a radially stable orbit. For this run the orbit was also given a small initial axial displacement (about 0.5 in.). As the run progressed the computer recorded the axial displacements, z, at intervals of once per sector. The resultant z-values are shown plotted in Figure 58 as a function of the number of revolutions. If there were no coupling

effects, this curve would be a smooth sinusoid of frequency $\nu_z = 0.3$ oscillations per revolution. The curve in Figure 58 shows, however, that the coupling effects are drastic. The ν_z value can be seen to shift in and out of the resonant value $\nu_z = 1/2$ and as it does so the amplitude of the axial motion grows rapidly. Thus, the 4-sector (tight-spiral) machine looked like a very bad risk as far as beam deflection goes. This conclusion corroborated the extensive work done at Harwell on coupling resonances.

A very similar computer run was made for the 3-sector field discussed above, (Fig. 54). The results here were strikingly different. The (once-per-sector) z-values followed a smooth sinusoid which was quite constant in amplitude and frequency over the length of the run (about 15 revolutions). This result was most encouraging. It was this feature, along with the others mentioned earlier by Cohen, his talk which lead the ORNL group to adopt a 3-sector geometry for their machine.